atmosphere

MDPI

Review

An Overview of Triggering Mechanisms and Characteristics of Local Strong Sandstorms in China and Haboobs

Zhaolin Gu [1,2,*], Yuanping He [3,*], Yunwei Zhang [1,2], Junwei Su [1], Renjian Zhang [4], Chuck Wah Yu [5] and Daizhou Zhang [6]

1 Department of Earth and Environmental Sciences, Xi'an Jiaotong University, Xi'an 710049, China; zhangyunwei@mail.xjtu.edu.cn (Y.Z.); sujunwei@mail.xjtu.edu.cn (J.S.)
2 Central Asia Research Centre for Atmospheric Science, Urumchi 830000, China
3 School of Atmospheric Sciences, Sun Yat-sen University, Guangzhou 510275, China
4 Institute of Atmospheric Physics, Chinese Academy of Sciences, Beijing 100029, China; zrj@mail.iap.ac.cn
5 International Society of the Built Environment (ISBE), Milton Keynes MK78HQ, UK; chuck.yu@btinternet.com
6 Faculty of Environmental & Symbiotic Sciences, Prefectural University of Kumamoto, Kumamoto 862-8502, Japan; dzzhang@pu-kumamoto.ac.jp
* Correspondence: guzhaoln@mail.xjtu.edu.cn (Z.G.); heyp27@mail.sysu.edu.cn (Y.H.); Tel.: +86-(029)-8339-5100 (Z.G.); +86-(020)-8411-5522 (Y.H.)

Abstract: The local strong sandstorms (LSS), similar to haboobs in Sahara and the North America, often occur suddenly, in tens of minutes during the late afternoon, and before dusk in deserts in China, causing a significant impact on the local atmospheric environment. The Sudan haboob or American haboob often appears in the wet season, followed by thunderstorm events. In contrast, the LSS in China appears most frequently in relatively dry season. The lack of observational data in weather conditions before their formation, during their development and after their disappearance have hindered our understanding of the evolution mechanism of LSS/haboobs. This paper provides a review of the current status and model studies on LSS/haboobs in different time and space to characterize the weather conditions and triggering mechanisms for LSS/haboobs occurrence, as well as highlight the subject for further understanding of LSS/haboobs. LSS are always followed by the occurrence of a dry squall. The interaction of dust radiation heating in the near-surface mixing layer with a mesoscale anticyclone air mass (cold-air pool) in the upper layer is the key process that leads to an LSS. Haboobs are followed by the occurrence of a wet squall. The release of latent heat due to the condensation of water vapor, involving moist convection and cold downdraughts, is the main driving force that cause the occurrence of a haboob. For a better understanding of the characteristics of the wind-sand two-phase flow and the mechanism of energy dissipation in LSS/haboobs, further accumulation of meteorological observation data and small-scale multiple-phase numerical simulations are required.

Keywords: local strong sandstorms; haboobs; squall; cold-air pool; convection

check for updates

Citation: Gu, Z.; He, Y.; Zhang, Y.; Su, J.; Zhang, R.; Yu, C.W.; Zhang, D. An Overview of Triggering Mechanisms and Characteristics of Local Strong Sandstorms in China and Haboobs. *Atmosphere* **2021**, *12*, 752. https://doi.org/10.3390/atmos12060752

Academic Editors: Keith Ngan, Chun-Ho Liu and Tetsuya Takemi

Received: 1 April 2021
Accepted: 6 June 2021
Published: 10 June 2021

1. Introduction

Sandstorms are severe weather events that can often be observed in the arid, semi-arid and adjacent regions. The frequency in the occurrence of sandstorms depends on the natural climatic variability and anthropogenic activities [1]. The sandstorms can be divided into regional sandstorms and local sandstorms according to their sizes. Regional sandstorms are caused by the synoptic-scale weather (such as the passage of cold front), ranging from hundreds to thousands of kilometers. Whereas, on the contrary, local strong sandstorms (LSS) are caused by meso- and small-scale local strong convections, usually ranging from tens to hundreds of kilometers [2]. High intensities of regional sandstorms or local sandstorms have been recorded, which were measured at all observation stations.

Regional sandstorms in China frequently occur in spring and have attracted significant interest from researchers [3–7]. For example, based on the meteorological data from 2001 to

2015, Yuan [5] analyzed the space-time distribution characteristics, weather system types and dynamic causes of sandstorms in some arid areas in China in the 21st century. He concluded that regional sandstorms mainly occur in spring and winter. Sandstorms in spring accounted for 97.6% of the total large-scale sandstorms in a year. Basha et al. [8] analyzed the spatial and temporal evolution of dust storms based on hourly observations at four stations in the United Arab Emirates during 1983–2014, and found most dust storms that lasted for about 5–11 h occurred in March and April.

In summer and autumn in China, there are frequently other dust events that occur in the desert. These mostly appear in the form of a LSS [9] or small dust devils [10–12]. In particular, the local strong sandstorms in northwestern China bear a striking resemblance to haboobs, which are dust phenomena found in the Sahara and North America. Haboobs can last for more than six hours with peak intensities of 0.5~1 h [13] often occur in northern and southern margins of the Sahara [14]. "An American haboob" [15] was introduced to describe dust storms that occurred over the arid southwestern United States, which are similar to Sudanese haboobs. Haboob phenomena have also been observed in the Middle East [16–18]. The sinking of cold air mass that push warm air near the ground to upraise was proposed to be the main cause of these events [19].

LSS or haboobs, generally associated with a strong wind, are complicated weather processes. A dust wall, usually up to hundreds of meters long, can form at the front of LSS/haboobs, and the propagating front is lobe-shaped. Airborne dust can strongly affect human life through respiratory and eye irritations, and pathogenic transmissions, and can cause damage to agriculture [20]. The occurrences of LSS and haboob are both attributed to severe convection weather processes, dry convection or moist convection. Sudan haboobs and American haboobs mainly occur in wet season with subsequent thunderstorm events, but heavy rain precipitation rarely occurs with LSS in China. This is because of the difference in relative humidity of squall line, which would be formed when cold air surges. LSS are always followed by the occurrence of a dry squall. The interaction of dust radiation heating near the ground with a mesoscale anticyclone air mass (cold-air pool) in the upper layer is the key process that lead to LSS. Haboobs are followed by the occurrence of a wet squall. The release of latent heat due to the condensation of water vapor, involving moist convection and cold downdraughts, is the main driving force that causes the occurrence of a haboob.

The basic features of LSS/haboobs can be drawn from conventional observation data and sometimes from mesoscale simulations. However, the lack of observational data on weather conditions prior to their formation, during their life span and after their demise have hindered our understanding of the evolution mechanisms of LSS/haboobs [21,22]. More research on the evolution of LSS or haboobs should be conducted based on a different scale simulation that combine the mesoscale meteorology simulation with micrometeorological methods, and with the computational fluid dynamics (CFD) method [9].

There are similar evolutions between LSS and haboob in the squall line of convection mechanisms and front shape in the mature stage, although they appear in different parts of the world with different meteorological conditions. The main aim of this study is to review the progress of research concerning the formation of LSS and haboobs to further clarify their similarities and differences, and provide suggestions for future investigations in strong sandstorms. In this short review, the observational studies of weather conditions of LSS and haboobs in space and time are described, and the numerical simulation of LSS and haboobs, including meso- and small-scale CFD simulations are presented. The triggering mechanism of LSS and haboobs is described and analyzed, and further research issues are also included for discussion.

2. Observation and Weather Diagnosis

2.1. Haboobs in Northern Africa, Middle East and Southwestern North-America

Northern Africa is the biggest export of dust in the atmosphere. The intensity of dust emission mainly depends on soil moisture and wind velocity [23]. Haboobs are a common

occurrence in northern Africa in the summertime, due to the existence of Sahara and Sahel Desert. The Sahel is between the Sahara (to the north) and the Sudanian Savanna (to the south), having a semi-arid climate. Haboob was firstly named in Sudan, which has the highest year-round frequency in dust emission [24]. Most commonly, the Sudan haboob occur in the afternoon, with wind speeds of 50~70 km h^{-1}, which carry dust to more than 1 km height and dust wall to 30~40 km diameter. The Sudan haboob is usually developed from thunderstorms. When a thunderstorm collapses, winds would change direction with a gust of wind rushes out of the storm, hitting the ground and uplifting all the loose dust.

Allen et al. [25] studied haboobs by high-resolution ground-based dust observations in the remote central Sahara for the Fennec project in June 2011. The results confirmed the importance of cold pools in dust emission and transport in the region. The structure in lidar backscatter profile showed that a raised "nose" was likely to be the leading edge of a haboob. Cowie et al. [24] explored the diurnal, seasonal and geographical variations of dust emission events and determined their thresholds in occurrence over the Saharan and Sahel region by long-term surface observations. The high year-round dust emission has a maximum of 18% occurrence in July, followed by August and June. A peak of dust emission was observed when a cold pool, caused by a squall line, reached the north of the Sahel during the summer. The occurrence of a haboob could be indicated by a jump in the frequency in dust emission (FDE). In Sudan, higher levels of FDE was demonstrated, which remained strong during the night when compared to the diurnal variation found in Sahel, suggesting a strong permanent presence of a dust emission in Sudan [24]. The consistent dip in emission just before, and after, sunrise indicated that the high dust emission at night in Sudan was caused by orographic flow in Nile valley. Zender and Kown [26] investigated 14 dust source regions and found that the rain precipitation could suppress or enhance dust emission on seasonal to inter-annual timescales. In most regions, precipitation as a main source of ground water helps form soil crusts, such as vegetation, which could reduce wind erodibility, and thus, dust emission on monthly timescales. In other regions, heavy precipitation increases the deposition of fine material due to flood-transport and desiccation, which could increase erodibility during subsequent dry periods (inter-annual lags). In arid Sudan, there are less rain precipitations and less seasonal variation in soil characteristics than in Sahel. Therefore, the seasonal variation of dust emissions in Sudan was less obvious than in Sahel.

Haboobs spawned by strong mesoscale downdraughts are also common in many parts of Middle East [17,18,27–29]. Miller et al. [18] conducted a United Arab Emirates Unified Aerosol Experiment (UAE^2) over the southeastern Arabian peninsula during the summer of 2004. They observed the haboob activity in this region via an assortment of satellite, radar, lidar and meteorological station network observation. In several cases, an environment favorable to convective activity supported the formation of haboobs. The dust lifted by the gust fronts of haboobs often travelled a distance greater than 100 km. The ensemble of haboob frontal passages, collected during this field campaign, produced 15-min mean wind speed increases of 10 m s^{-1}, pressure rises of 2 mb, humidity increases of 15%, and temperature fall of 7 °C.

Mamouri et al. [17] examined the meteorological processes of a haboob event occurred over the Cyprus region in September 2015. The observations were based on satellite observations of aerosol optical thickness and surface particle mass (PM_{10}) concentration measured at four sites in Iraq, Iran, Turkey and Syria. The findings showed that a thermal low formed over Syria on 6 September 2015 was associated with a strong cloud convection and provided favorable conditions for the generation of a haboob along the borders between Iraq, Iran, Turkey and Syria on 7 September 2015. Additionally, the changes in land use and surface characteristics, associated with the civil war in Syria and other political conflicts in that region, probably enhanced the efficiency of dust emissions thereby causing the occurrence of the haboob.

The American haboob, as has occurred in southern Arizona, is typically caused by downdraughts from thunderstorms that have been developed over the mountain region.

There have been many reports of haboobs due to the occurrence of three major outflow systems in Phoenix, Arizona, USA, in 2011. On 5 July 2011, Phoenix haboob was described in detail in the US National Weather Service forecast office report [30]. The high surface winds that trigger the haboob, arose from thunderstorm outflows and the downburst of cold air, leading to the formation of a cold-pool atmospheric circulation over the northern Phoenix. The cold pool outflows are generated by the evaporation, sublimation and melting of hydrometeors in a thermally unstable atmosphere. The convectively generated cold pool in a typical haboob would have depths of approximately 1 km [15,31]. However, other studies showed depths of up to 4 km [32]. These cold pools form the key precursor to the mechanism that generates strong winds with a consequent dust uplift from the surface to cause the haboob occurrence [31,33–35].

Raman et al. [36] used satellite, radar and ground-based observations to determine the state and fate of a haboob, which occurred in Phoenix on 5 July 2011. Their findings suggested that the haboob was a result of strong outflow boundaries from thunderstorms, which have been developed in the southeast of Tucson. Thunderstorms, lasting about two hours, usually occurred after these dust storms. The data of aerosol optical depth (AOD) and daily-average PM_{10} on 6 July 2011 were also analyzed to clarify the impact of 5 July 2011 haboob. High AOD values were observed across Phoenix on 6 July 2011. An enhanced dust loading was observed in the northwest of Phoenix, suggesting that the dust transported by the Phoenix haboob was less than a day. These kinds of dust storms always have squall lines and are composed of numerous cells. The leading edge of the dust front was ~160 km wide with a dust wall of ~2.4 km [22], which contributed to an intensified downdraught pattern that swept through the valley.

The occurrences of haboobs over the desert areas in northern Africa, Middle East and southwestern North-America were both driven by cold pool outflows that act as density currents and are often produced from the downdraughts of moist convective. The moist convections are generated by the generation, melting and sublimation of hydrometeors. The passage of a cold pool is generally associated with a short-lived pressure rise, an increase in wind speed and a shift in wind direction.

2.2. Local Strong Thunderstorms in Northwestern China

The LSS in the northwestern China, usually occur with an instantaneous wind speed of more than 25 m s^{-1} and a visibility of less than 50 m. The LSS are mostly caused by a strong near-surface thermal convection in a small scale over a short duration, usually in tens of minutes, occurring in the period of late afternoon to dusk [37]. In the convection, the variation of the ground air temperature causes a variation in the wind speed in the vertical direction. Usually, the desert has a large temperature gradient in the vertical direction in the afternoon, resulting in a strong convection of local sandstorms [38,39]. The interaction between atmospheric weather conditions (e.g., cold front or upper-level trough transit) and the instability of the local atmosphere during the developing process of the dry squall line would trigger the appearance of a LSS [40,41]. However, Sudan haboob or American haboob are generally influenced by wet squall line, which cause strong thunderstorms and heavy precipitation.

Taklimakan Desert, the largest desert in China, is an important source of global dust aerosols. Yang et al. [42] established a Desert Environment and Climate Observation Network (DECON) for field research of dust-storms in the Taklimakan Desert region. Soil moisture and soil temperature were reported as important factors that could influence dust emissions. Through the statistical analysis of meteorological data, Ma et al. [9] reported that the frequency and time duration of a LSS occurrence are unevenly distributed each month. The highest frequency and longest duration occur in summer. Wind, as a kind of power, is the energy source for the sandstorm movement. The structural characteristics of a wind field could directly affect the near-surface sand-blown and vertical transportation.

Figure 1 shows photographs of two LSS occurred in Xingjiang Province, and Inner Mongolia Autonomous Region, respectively. LSS events often appear in Xinjiang, Gansu,

Inner Mongolia and other desert source areas and desert edge areas in the north-western part of China, irrespective of the differences in physical properties of the desert surface matter in different regions. During the occurrence of a LSS, the sky could be sunny or cloudy. The sandstorm was caused by the coupling of the upper mesoscale cold pool and a strong heat convection on the ground in the afternoon and before dusk. The sand wall of the sandstorm front is about 100 m height. The visibility within local sandstorm plumes is less than 50 m. The frontier of the sand wall is clearly distinguishable and the cloud layer above is stable. The rising altitude of a sandstorm during the occurrence of a LSS is not high and its horizontal transportation distance is short. The impact of a local sandstorm is limited, ranging from tens of kilometers to hundreds of kilometers.

(**a**) (**b**)

Figure 1. The fronts of two local sandstorms occurred (**a**) on 6 April 2019 in Alar City, Xinjiang Province, China (http://news.2500sz.com/doc/2019/04/08/424594_4.shtml, accessed on 12 December 2020); (**b**) on 2 August 2017 in E-Ji-Na County, Inner Mongolia Autonomous Region, China (https://baijiahao.baidu.com/s?id=1574686840525110&wfr=spider&for=pc, accessed on 12 December 2020).

Historically, LSS were extraordinarily called "black storms" [43–45]. On 5 May 1993, in the north-western arid region of China, including Hexi Corridor in Gansu Province, Inner Mongolia Autonomous Region and Ningxia Autonomous Region, there was a large-scale strong sandstorm that had, so far, rarely been observed in history. In that event, the strong sandstorm was observed in the local region, also known as parts of "93.5" black storm. There have been several studies on LSS, using the mesoscale numerical simulation data of a "93.5" black storm and the energy equation of the moisture perturbation [46]. The analysis of the development process revealed that the tremendous release of the potential energy from the moisture perturbation in the planetary boundary layer (PBL) was the main energy source for the rapid development of the black storm [47]. The simulation using the NCAR MM4 model with a high-resolution PBL parameterization indicated that the development of the black storm was directly related to the formation and development of a mesoscale cyclone [48]. The formation, development and columnar vertical structure of the total vorticity source were consistent with the vorticity of mesoscale vortex during a black storm. Besides, the time that the cold front reached the middle of Hexi Corridor in Gansu Province was the most unstable period of the atmospheric boundary layer. The ascending motion of the cold front could trigger the convective instability energy to release quickly, thus, resulting in the occurrence and development of the squall line system [40,41]. Takemi et al. [49,50] studied the "93.5" black storm by mesoscale observations and found that a strong cold pool outflow was associated with a front system, which was thus, developed in a synoptic-scale cyclone system. In fact, the cold outflow is often observed in haboob events [15,51]. In this black storm event, almost no rain was observed on the ground level. This is in contrast with those haboobs found in Sudan and America that are typically developed in humid regions [15,51].

Using conventional observation data and satellite images, Ma et al. [52] studied a strong sandstorm event on 18 April 1998 in the northern Tianshan Mountains, Xinjiang

Autonomous Region of China. Their results indicated that the wind, pressure, temperature and humidity, all were abruptly changed when LSS were passing through weather stations. The dust wall was almost isothermal with the horizontal thickness of about 4–9 km. There was a deep near-surface mixing layer prior to the formation of LSS in drought region induced by the surface heating. After the passage of a short-wave trough, wind began blowing from a cold-air region to a warm-air region, i.e., cold advection, which triggered a dry squall line.

The analysis by Li et al. [53] of the variation of meteorological parameters of twelve LSS in the east of Hexi Corridor in summer (June–August) during 1971–2018, also showed an increase in the ground temperature throughout the period from the afternoon to the evening, often leading to a convective instability of the atmosphere. Therefore, summer sandstorms mainly occured in the local thermal convective condition induced by small- and medium-scale weather systems. The meteorological parameters in the high-altitude and near ground could change significantly during their life span of a LSS. Before the occurrence of a LSS, there is low atmospheric humidity in the whole troposphere, cold advection in the upper level, obvious warming in the mid-lower level, thermal depression and high air temperature above ground. This warm dry air in the lower level assists in the development of convective activity. During the outbreak and transmission of a LSS, the temperature descends and the humidity increases both in the high-altitude and near ground.

The heterogeneous increase of the near-surface air temperature would usually produce thermal convective cells in the mixing layer [49,54]. There is a deeper mixing layer in the summer and autumn than in other seasons. While, the mesoscale anticyclone air mass (cold-air pool) in the summer and autumn may not be deeper than in winter and spring. The complementarity of the thin cold-air pool with a deep mixing layer favors the occurrence of local sandstorms. The strength of the vorticity of the cold-air pool determines whether the near-surface convection could be induced into the dry squall line and the strength of the dry squall line of a local strong sandstorm. In summer and autumn, deserts at low latitude areas experience plenty of solar radiation, thus, producing warm cells (low-pressure) by a strong sensible heat of the atmosphere in desert areas [55]. Such low-pressure is, in general, characterized by an upward movement inside the hot air column above the desert source area and a downward movement around it. If there is no daily change in the thermal condition in the boundary layer over the desert, the wind field corresponding to the stable pressure gradient and the Coriolis force becomes a cyclone in the near-surface of a hot low-pressure layer and an anticyclone in the high-altitude of a high pressure [56,57]. The movement of a high-level low-temperature anti-cyclone, a kind of cold air mass, is the source of vorticity for the downwind zone.

In conclusion, the basic weather conditions for the occurrence of a LSS are as follows: A cold-air mass with certain helicity propagates into desert source areas; a strong thermal convection is generated on the surface of a desert source area, forming a mixed layer of atmospheric thermal convection cell structure. In the development of the near-surface thermal convection, the variation of ground air temperature difference would cause a change in wind speed. In theory, the cold-air mass and surface mixed layer are independent weather processes, and can exist in four seasons over desert areas. Understanding how a cold-air mass interacts with the ground deep mixing layer, and consequently induces a strong sandstorm, needs to be further clarified.

3. Different Scale Numerical Simulation Methods of LSS/Haboobs

3.1. Mesoscale Simulation Methods of Dust-Uplift by LSS or Haboobs

LSS and haboobs are local and mesoscale atmospheric density currents that mobilize huge amounts of dust that create a propagating dust wall [16,58]. The scale of the processes that participate in the generation of such atmospheric density currents range from a synoptic scale to a mesoscale and local scale. Many coarse-resolution models have been used to characterize the monsoon circulation and synoptic-scale dust emissions [59–61]. These

large-scale models could capture the geographical distribution of LSS/haboobs and their seasonal cycle. However, these small-scale physical processes, including the development of near surface vortices, the variation of temperature, humidity and wind, as well as the dust lifting and transport are not well captured by synoptic-scale models [62,63]. High resolution simulations of the triggering and evolution of LSS/haboobs require dust models that are able to describe deep convection and PBL processes [57]. Numerical modelling studies can provide crucial evaluation and forecasting of the amount of dust emission and transport. Mesoscale simulation models have been developed worldwide for characterizing dust storms, rather than large-scale models due to the problems with resolving convective events and associated wind gusts. The mesoscale models can describe the effect of convective-scale up-draughts and downdraughts, as well as mesoscale circulations within mesoscale convective systems based on the three-dimensional transport of mineral dust [64].

3.1.1. Mesoscale Simulation Methods of the Wind Field Laden with Haboob Sand

The forecast of the small scale of a micro-burst generating haboobs is complex and difficult. However, understanding the occurrence of these dust storms would enable the development of simulation methods. These haboobs generally have a mesoscale high-pressure area. The cool dense sinking air and heavy rain generate strong winds after the thunderstorm [22]. The evaporation of the rain in the upper level above the ground arising from the dry near-surface can enhance the downdraught through the cooled air. The high-velocity horizontal wind continues, thereby causing a huge dust uplift in the dust source area, leading to the formation of a haboob.

Sundram et al. [65] simulated dust storm events in central and eastern Washington by using a 4 km resolution prognostic meteorological model MM5, coupled with a CALMET/CALGRID model and a dust emission module EMIT-PM, which provided an excellent simulation of strong dust storms, but could not simulate dust plumes or smaller storms. Almost half of the modelled summertime dust emission in the Western Africa can be generated by haboobs, as shown by mesoscale multi-day convection-permitting simulations. However, in the global parameterized convection model, this dust emission was not included in the evaluation [62,66,67]. The mesoscale convection-permitting model with 4, 12 and 40 km horizontal grid-spacing has been developed to investigate haboobs in Western Africa [62] and the model with 4 km horizontal grid-spacing was used to investigate haboobs in the United States [22]. A coupled atmospheric-air quality RAMS/ICLAMS model was used to study the haboob associated with density current in Africa and the Middle East [16].

The haboob in Phoenix in the period 5–6 July 2011 was used for a high resolution numerical simulation, and to forecast haboobs and other similar events [30,68,69]. Foroutan and Pleim [69] developed a new regional-to-global model by incorporating the effects of subgrid wind variability and cold pool outflows. This updated model successfully simulated the haboob that hit Phoenix on July 2011. Haboobs with intense vertical mixing require non-hydrostatic mode models to characterize and predict the event. The dust sources in the southwest of the United States mainly arise from ploughing of agricultural fields that produce a large amount of dust, which scatters over the region.

A 4 km high-resolution numerical model NMME–DREAM was developed by Vukovic et al. [22] to simulate the American haboob. This atmospheric-dust model is coupled by linking the atmospheric numerical weather prediction model, NMME with a dust regional atmospheric model DREAM to simulate the atmospheric dust cycle. DREAM dust transport parameterization consists of a viscous sublayer between the surface and the lowest model layer [70], with a similar mass–heat–momentum exchange between surfaces for mass dust particle transport over the desert region [71].

The NMME–DREAM model is for the resolution of the Euler-type partial differential nonlinear equation for dust mass continuity. The evaluation conducted by the atmospheric-dust model simulates the weather condition that was driving the dust storm.

The atmospheric-dust model shows the arrival of a cold front was one hour late during the haboob in Phoenix, Arizona on 5 July 2011 [22]. A horizontal vortex was visible within the cold air in the frontal area of streamlines and the rotation center was at around 1 km altitude. The analysis by the dust-storm model showed a peak of dust concentration in the south of Phoenix was up to ~2500 μg m^{-3}. However, the model underestimated the PM_{10} concentration in comparison to measurements. In addition, the dust model that incorporates the subgrid wind variability and lightning assimilation could also underestimate the PM_{10} concentration [69]. This underestimation might be due to the difference of soil moisture between the reality and the modelled. Further investigation of the atmospheric-dust model and dust sources would be needed to clarify the parameterization of the dust cycle and would require further measurements [22].

Weather Research and Forecasting-Chemistry coupled model (WRF-Chem) as a mesoscale meteorology model also has been widely used in forecasting strong dust events [28,30,68,72,73]. Karegar et al. [72] simulated the haboob events in east of Iran by the WRF-Chem model. The model was run for 10 and 30 km spatial resolutions, and results revealed the formation of haboob was affected by local geographical properties especially topography features. Local factors could reduce the model resolution and the intensity of the haboob would be sharply reduced. Raman et al. [30] evaluated the performance of WRF-Chem model in simulating the 5 July 2011 Phoenix haboob using retrievals of aerosol optical properties and mass concentrations from satellite instruments, in conjunction with available surface $PM_{2.5}$ and PM_{10} concentration measurements from in-situ observation sites. The results showed that the WRF-Chem model was able to capture the spatio-temporal pattern of the haboob, but largely underestimated the magnitude of surface dust concentration and aerosol optical depth. The underestimation of the surface dust concentration was mainly manifested in the coarsest model bin (5–10 μm), which became the most produced during sand-dust weather. In addition to soil moisture, the model cutoff diameter should also be taken into account in the improvement of mesoscale haboob models.

3.1.2. Mesoscale Simulation Methods of Dust-Uplift by LSS

The mesoscale simulation of LSS in China generally adopted a non-hydrostatic cloud model, which is an advanced regional prediction system [74,75]. The non-hydrostatic cloud model provides an effective tool for research and a system suitable for explicit prediction of convective storms. A squall line, having a forward-extending cloud region in the upper level and a well-developed cold pool, was observed over a desert region on a "93.5" black storm event [49]. The squall line environments have a characteristic low moisture content, high level of free convection and low convective available potential energy (CAPE) over the arid region in China.

Takemi and Satomura [50] investigated the development of squall lines in dry environments with a mixed layer in the lower layer by using a two-dimensional non-hydrostatic cloud model. The depth of the mixed layer in the model was set to 4375 m, which was estimated from the depth of maximum mixed layer on a "93.5" black storm event [49]. During the mature stage of this simulated squall line, a cold-air pool was well-developed. On the one hand, the air parcels, originating from the upper level of the mixed layer ahead of a surface cold-air pool, were raised to the upper troposphere, driven by a vertical pressure gradient force and then by a positive buoyancy. On the other hand, the air parcels, originating in the lower level of the mixed layer, were forced to move rearward, as they were driven by the rearward pressure gradient force. The low pressure just above the surface cold pool had a critical role in determining the trajectories of air parcels within the mixed layer. In addition, the sensitivity of squall lines to low-level thermodynamics structure, including mixed layer depth and vertical profile of moisture, was significantly analyzed. The cold-air pool and the vertical distribution of CAPE were found to be critical for developing and maintaining squall lines in dry environments. The convective systems,

such as LSS over the arid regions in China, could be developed and maintained under environmental conditions with a deep mixed layer and well-mixed moisture profile.

Additionally, an integrated operational dust numerical prediction system, applicable for East Asia, has been developed by the National Meteorological Centre in China [76]. The system includes a mesoscale meteorological model, a land surface model, a wind erosion scheme, a sand transport model and a geographic information system. The modelling system can predict the basic characteristics of dust events and also offers predictable information about the whole process, including origination, development and weakening of the dust episode [77].

3.2. CFD Simulation Methods of Dust-Uplift by LSS or Haboobs

Affected by the initial field, boundary conditions, dust-uplifting process, topography, underlying surface condition and soil moisture scheme, the mesoscale numerical results of dust storms inevitably have some errors in their order of magnitude and the spatial distribution of dust aerosols. To accurately predict the occurrence of extremely strong sandstorm, the multi-scale triggering mechanism and initial conditions of the sandstorm process must be fully evaluated. The small-scale processes (e.g., turbulence) in LSS/haboobs should be captured for clarifying the triggering mechanism and evolution processes of LSS/haboobs. Therefore, high-resolution numerical models are required for the accurate simulation of small-scale processes in haboobs.

Large-eddy simulation (LES) and Reynolds-averaged Navier-Stokes (RANS) are two computational fluid dynamics (CFD) methods for the simulation of turbulent flows. The Large Eddy Model (LEM) incorporating the subgrid-scale (SGS) model based on the Smagorinsky-Lilly approach, is often used in a wide range of boundary-layer simulation as a non-hydrostatic model [78]. In LES, large scale motions of the flow can be calculated, and the effect of smaller scales can be simulated using SGS model [79]. Although LES could better capture the fluctuation of the flow field in comparison to RANS, it is computationally more expensive [80]. In fact the RANS method is sufficient for most high-resolution numerical simulations of turbulence, as it can supply adequate information about the turbulent process [81].

3.2.1. LES Simulation of Dust-Uplift by Cold Pools

The transport and evolution of dust in an idealized haboob density current was successfully simulated by Huang et al. [82] using LEM that includes incomprehensible Boussinesq formulation for solving the turbulence in the cold-pools. The simulation did not consider moisture processes, as the model would never reach saturation due to the cold pool was generated by an idealized cooling. More small-scaled turbulence was captured for runs that increase the model horizontal resolution from 1.0 to 0.1 km, and about twofold reduction in the accumulated dust uplift was presented. A high resolution simulation model could better resolve turbulence for the study of haboobs [82].

The LES simulation of one idealized cold pool indicates that convection-permitting models are suitable for haboob parameterizations. The modelling of peak winds within any haboob could be evaluated by a better resolution of eddies. The understanding of interactions of cold pools with near-surface mixing layer by modelling would be clarified by further accurate simulation of cold pool outflows [82].

3.2.2. RANS Simulation of Wind Induced LSS by a Cold Pool

Previous observations and theoretical models have shown that the passing of a cold pool in the upper level of atmospheric mixing layers is likely the key process that triggers the occurrence of a LSS/haboob [22,47,56]. The Reynolds Averaged Navier–Stokes (RANS) method was used in these studies. He et al. [19] used the numerical calculation to clarify different stages of the evolution of an LSS. Once the intrusion of an upper cold-air pool was included, a mixing layer appears, its sinking leads to the downdraught of a cold pool, entraining convective cells in the mixing layer into massive swirling convective cells. The

temperature difference between the thermal convective cells and the cold pool at the upper layer plays a decisive role in the formation of LSS.

Figure 2 illustrates the characteristics of LSS at the fully developed stage in the RANS simulation conducted by He et al. [19]. Figure 2a shows that the initial temperature structure in layer by layer is completely destroyed, forming a large number of thermal convective cells. The deep convection of thermal convective cells is the key to forming LSS [49]. The temperature near the ground declines by more than 10 K, in agreement with previous observations [2,16,40,49,83,84]. Figure 2b is the horizontal velocity distribution at 1 km height at the fully developed stage with a wind speed of about 10–30 m s^{-1}. The velocity contours indicate the appearance of many vortices with different diameters [19]. In particular, sub-vortices (secondary vortex) subsequently occur within the main vortex. The sub-vortices are created along with the downdraught of a centered cold pool. Besides, a strong shear flow appears around the periphery. Then, the entire development region becomes dominated by the swirling downdraught in the center and the swirling up-draught at the periphery. Also, there is a strong shear in the airflow field, which leads to a turbulent field. In fact, the existence of these sub-vortices indicate the decay of a LSS. Numerous vertical sub-vortices airflow would generate "waves" forming several "lobes" that appear at the front edge of a LSS [34]. The haboob vortices in different intensities have been reported in sandstorm observations [85–87].

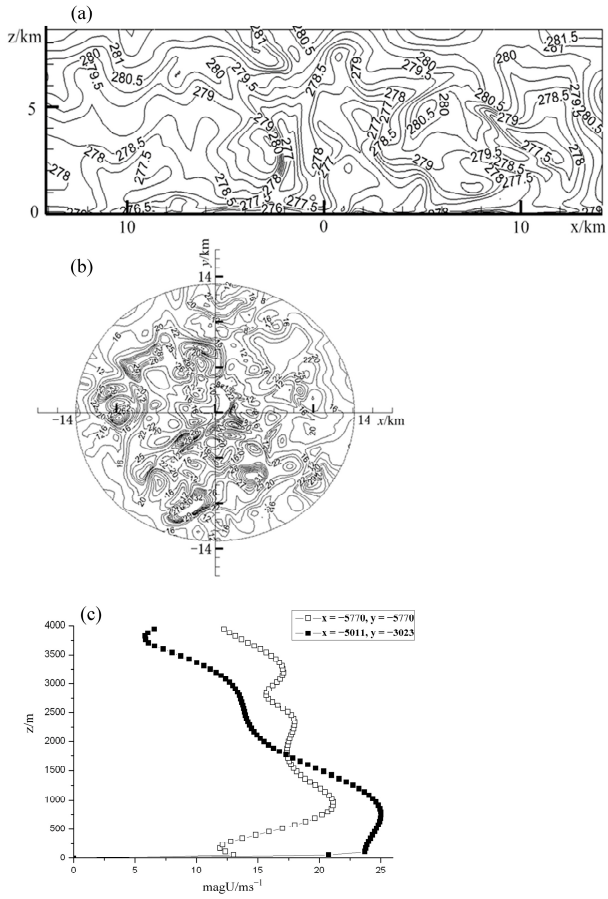

Figure 2. Air flows field at the full development stage (**a**) Air temperature in the central vertical plane z-x; (**b**) Horizontal velocity contours (m s^{-1}) in the x-y plane, z = 1000 m. The appearance of many vortices with different diameters would generate "waves" forming several "lobes" that appear at the front edge of a LSS. (**c**) The resultant wind velocity profiles at different altitude of two positions (x = −5770 m, y = −5770 m, and x = −5011 m, y = −3023 m) around the cold pool center. The remarkable feature of these velocity profiles is their "lobes" shape, which contributes to dust uplift from the surface (the simulation was conducted using RANS model by He, Y., 2020).

Figure 2c shows the resultant wind velocities at two positions during the fully developed stage. The distinctiveness of this front in cross section is its "nose-like" shape, in which the gas circulation velocity exceeds the forward speed of the front and its frontal pressure is very large. The dust uplift is formed by the horizontal vortex within the cold air at the nose-like leading front, which is consistent with the reported observation [25] and the simulation by convection-permitting model [62]. A higher wind velocity in a LSS carries and discharges the dust farther away.

The LES and RANS simulations conducted by Huang et al. [82] and He et al. [19] both used an idealized cooling in their modelling to generate the cold pool. The turbulence structure in LSS and haboobs are well-understood. However, moist processes were not considered in their numerical models. In fact, the environmental humidity for the formation of LSS and haboobs are different. Besides, several streams of cold air came together are common in synoptic pattern. Future studies on small-scale simulations should consider moist processes and the presence of multiple cold pools.

4. Triggering of LSS and Haboobs

LSS/haboobs are caused by meso- and small-scale weather phenomena, such as local strong convection, usually ranging from tens to hundreds of kilometers. The interplay of dust radiation heating and local atmospheric instability in the growth process of the squall line are responsible for triggering LSS/haboobs [40,41]. In fact, Africa or American haboobs often appear in the wet season, but LSS in China mostly appear in the dry season. Therefore, there are differences in the triggering conditions between the haboob and LSS, which are closely related to the relative humidity of the formed squall line in the invasion of the cold air. The generation of a LSS is mainly driven by the thermal convection, while the haboob is driven by the moisture convection and the thermal convection. The main similarities and differences between LSS and haboobs are listed in Table A1 (see Appendix A).

The difference in the surface albedo could result in an uneven distribution of air temperatures on the earth. Desert and wilderness areas have high surface albedos, such as 0.35 in desert and 0.25 in wilderness areas, so that the height of the near-surface mixing layer are usually larger in deserts than in other areas. The ascending rise of warmed air causes a convergence of the surrounding air, producing a local thermal circulation. Due to the stable atmospheric stratification, the local rising of air is usually presented in a well-organized convective cell structure [88,89]. For open convective cells, the air sinks at the center of the convective cell and then rises in the surrounds of the center [90,91]. Hexagonal clouds are often formed in up-draught areas of open convective cells [54].

Once a mesoscale cold air enters into the upper layer of the mixing layer, the down-draught of the cold air would induce the ground convective cells into an unstable movement. The cellular convection would then transformed into a strong convection of massive helical cells. The movement of swirling convective cells is similar to a tornado or a dust devil. In order to maintain the stability of these swirling convective cells, the ascending velocity at the leading edge of the swirling convective cells increase significantly, and lead to an unstable vertical airflow of convective cells, and consequently, a large-scale instability of a near-surface mixing layer [10]. The fall of the cold air tends to concentrate on the gust front as the cold front advances, forming a density current head, as shown in Figure 3 [92].

Figure 4 depicts the morphological characteristics of the front edge of a LSS that occurred on 5 May 1993 in the northwestern China [44]. Similar to the entrainment mechanism of particles in the dust devils [54], the uprising dust particles from the ground were projected by the swirling air flow in the azimuthal area of swirling convective cells, forming a nose-like front, as illustrated in Figure 4a [44]. At the same time, particles in different sizes can be stratified under the helical up-draught of swirling convective cells [93]. The stratified dust particles exhibit the shallow and uneven layers of a LSS, as shown in Figure 4b. Fine particles are shown to concentrate in the upper layer (zones G and H in Figure 4b), medium size particles concentrated in the lower level (zones A and B), and coarse particles circulated near the ground. Due to different properties of light

reflection and absorption according to particle sizes, the sand wall appeared in layers in different colors at the leading edge of a LSS, with the upper yellow layer of fine particles, the middle red layer of medium size particles and the lower grey-black layer of coarse particles occured near the ground [44]. In fact, the observation of LSS on 5 May 1993 showed that the dense sand wall was about 0.3 km high, while the dust layer was higher, about 0.7 km. Moreover, prior to the occurrence of a LSS, the warm air in the near-surface layer would became very unstable, and during the development stage, the sand inside the sand wall began tumbling. The weather process with a severe convection, produced the characteristics of a squall line [40,41].

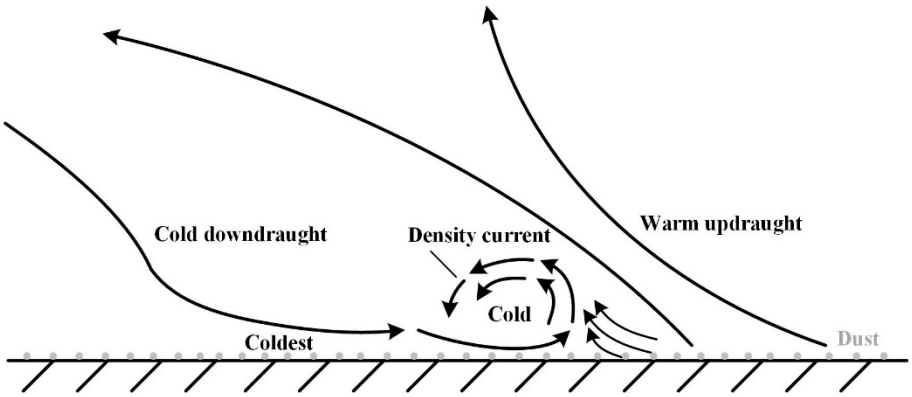

Figure 3. Schematic diagram of the front lobe of a dust storm. A downdraught of the cold air that spreads out along the ground and moves forward to form a density current pick up loose dust and sand from the surface. The dense cold air pushes up warmer air, which it meets, thereby reinforcing the warm up-draught (Modified from Idso, S.B. 1976, pp. 108–114).

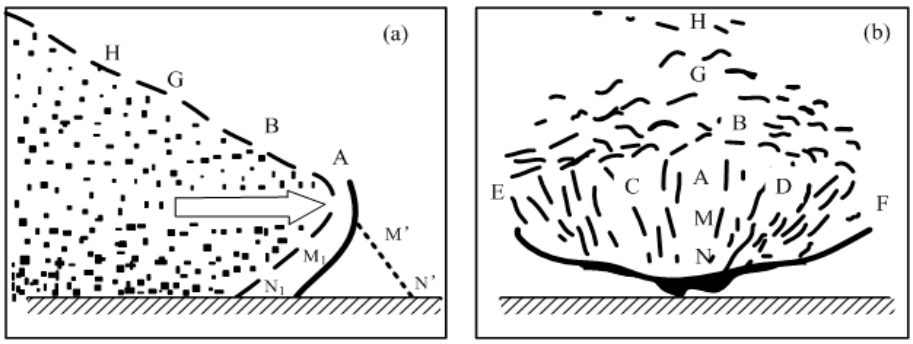

Figure 4. The front features of a LSS event. (**a**) Side view diagram. Due to the ground friction and other retardation, the wedged front of the cold air is not directly grounded like a dashed line AM'N', but is shaped like a nose (line BAMN) that folds backwards. A is the nose tip. (**b**) Main view diagram. The front view is the CD portion of the nose tip of the cold air, which is just a small segment of the curved cold air pushing forward. To the left and right sides to E and F, up to G and H, down to M and N, the dense sand edge and its inner rolling gradually become blurred. The uneven layers, deep or shallow, are caused by separated process of different sized dust particles (The Figure was reproduced from Lu, Q. and Yang, Y.L. 2001, p. 158).

The above analyses agree with the observations of a LSS. LSS is a motion of massive swirling convective cells, caused by the interaction of convective cells in the near-surface mixing layer with the upper cold air pool [94,95]. The triggering of a LSS is not only the full development of convective cells in the mixing layer, but also the transitioning of a mesoscale anticyclone with a certain vorticity (helicity) in the upper mixing layer. In particular, the horizontal movement of the anticyclone or the cold pool should be within a certain range to induce the transition of the simple honeycomb convective cell structure to the massive swirling convective cell structure. This produces larger and longer-lived

downdraughts, which subsequently leads to cold air spreading over much larger areas. The cold airflows in LSS and haboobs have very similar structures as they both clearly display similar lobes, clefts, billows and nose structures.

5. Summary and Perspective

LSS and haboobs usually occur in the sand source areas or their marginal areas. Their basic features and characters could be drawn from conventional observation data and sometimes by mesoscale simulations. LSS and haboobs can occur throughout the year, but LSS are more common in dry season and haboobs are more common in the wet season. LSS and haboobs occur suddenly and locally in the afternoon or evening, in short duration. They can also cause a significant impact on the local atmospheric environment quality. The basic meteorological conditions include the convective cell flow in the near-surface mixing layer in desert regions or close to deserts. The transitioning of a mesoscale anticyclone or a cold air pool can occur over the desert. The squall line and the sand-blown process are distinctive characteristics of LSS and haboobs. The occurrence and evolution of thermal convection and convective cells in the desert area favor the occurrence of LSS and haboobs.

Much progress in model simulation has been made, such as the mesoscale convection-permitting simulations (3.75 km grid-spacing) of haboobs in the USA, the CFD simulations for microscale behaviors. The CFD simulation includes the LES simulation of haboobs induced by a cold-air pool and the RANS simulation of LSS induced by a cold-air pool. The CFD simulation for LSS showed that, after a large dust storm has fully developed, there are often many subsequent sub-vortices (secondary vortices) in its convection field. The distribution of wind velocity in these vortices is consistent with the "nose-like" shape of LSS. The subsequent sub-vortices can result in a quick dissipation of energy of LSS, which decay and retard the occurrence of the LSS. The simulation results are consistent with observations of the LSS, indicating the critical role of the invasion of the cold air pool in the upper layer and the formation of convective cell structure in the mixing layer. The following aspects need to be addressed in further studies, in order to deepen our understanding of the triggering mechanism and evolution of LSS and haboobs.

1. Observations of meteorological factors in desert and marginal/periphery areas with high-resolution time-series are necessary to obtain the basic information relating to the evolution of LSS or haboobs.
2. The development of mesoscale anticyclone or cold pool as the vorticity to trigger LSS or haboobs should be carefully investigated. The intensity and size of a cold pool vorticity usually determines whether convective cells in the mixing layer can develop into LSS or haboobs.
3. Small scale, high-resolution CFD numerical simulations should be further developed to investigate the interaction of the upper cold pool with the deep mixing layer for the evolution of haboobs or LSS that cause an up-draught of the air. The simulation of wind-blown gas-solid two-phase flows further supplement our understanding of the uplifting of sand particles by LSS or haboobs and rapid energy dissipation.
4. Appropriate numerical simulation analysis method is necessary to determine the dynamic evolution of the downdraught of a cold pool acting with convective cells in the mixing layers. This provides useful information to analyze the transformation of simple thermal convective cells to massive swirling convective cells. The numerical simulation analysis also provides the statistical diagnosis of parameters in the low-pressure zone for the formation of swirling convective structure and the uplifting of sand.

Author Contributions: Supervision, organizing, Z.G.; writing—original draft, Y.H.; writing—original draft, Y.Z.; writing—original draft, J.S.; summarizing, R.Z.; writing—review and editing, C.W.Y.; writing—review and editing, D.Z. All authors have read and agreed to the published version of the manuscript.

Funding: This study was financially supported by the China Postdoctoral Science Foundation (Grant No. 2020M672944) and the Central Asian Research Fund for Atmospheric Science (Grant No. CAAS201702).

Conflicts of Interest: The authors declare that they have no conflict of interest.

Appendix A

Table A1. Comparison of LSS and haboobs.

	Characteristics	LSS	Haboobs
Similarities	Wind speed	>25 m s^{-1} [24,49]	
	Visibility	<50 m [27,49]	
	Duration	Tens of minutes [24,37]	
	Shape	Dust wall, lobe-shaped [34,44]	
Differences	Cause	Thermal convection [49]	Moisture convection and thermal convection [17]
	Region	Northern Africa [23–26]; Middle East [17,18,27–29]; Southwestern North-America [22,30,32,36]	Northwestern China [9,37–50,52,53]
	Season	Dry season [49]	Wet season [36]
	Weather	No rain [49,50]	Thunderstorms and precipitation [15,51]
	Mesoscale simulation	Two-dimensional non-hydrostatic cloud model [50]; integrated operational dust numerical prediction system [77]	Mesoscale multi-day convection-permitting simulations [16,22,62]; NMME–DREAM model [22]; WRF-Chem [28,30,68,72,73]
	Small-scale simulation	RANS [19]	LES [82]

References

1. Chen, F.; Chen, S.; Zhang, X.; Chen, J.; Liu, J. Asian dust-storm activity dominated by Chinese dynasty changes since 2000 BP. *Nat. Commun.* **2020**, *11*, 992. [CrossRef] [PubMed]
2. Zhang, G.; Li, X. Research status of sand-dust storm observation and classification standard. *J. Desert Res.* **2003**, *23*, 586–591. (In Chinese)
3. Pan, Y.Z.; Fan, Y.D.; Shi, P.J.; Gu, X.H. Spatial variation and seasonal distribution of dust-storm in China in resent 50 years: A preliminary study. *J. Nat. Disasters* **2003**, *12*, 1–8. (In Chinese)
4. Yin, X.H.; Wang, S.G. Fractal characteristics and trend forecast of dust—storms and severe-dust—storms in northern China. *J. Desert Res.* **2007**, *27*, 130–136. (In Chinese)
5. Yuan, G. Characteristics and cause of the sandstorm in Inner Mongolia in 2001–2015. *J. Desert Res.* **2017**, *37*, 1204–1209. (In Chinese)
6. Zhao, M.R.; Yan, D.T.; Li, Y.Y.; Zhang, C.S.; Hu, L.L. Change characteristics of sandstorm frequency and its causes in 2001–2010 over Minqin, Gansu, China. *J. Desert Res.* **2013**, *33*, 1144–1149. (In Chinese)
7. Zhao, M.; Liu, M.; Qian, L.; Wang, S.; Li, Y. Variation characteristics of sandstorm from 1871 to 2010 over Minqin oasis and its cause. *Desert Oasis Meteorol.* **2013**, *7*, 35–39. (In Chinese)
8. Basha, G.; Ratnam, M.V.; Kumar, K.N.; Ouarda, T.; Kishore, P.; Velicogna, I. Long-term variation of dust episodes over the United Arab Emirates. *J. Atmos. Sol. Terr. Phys.* **2019**, *187*, 33–39. [CrossRef]
9. Ma, J.; He, Q.; Yang, X.; Huo, W.; Yang, F. Characteristics analysis of regional and local sandstorm over the hinterland of Taklimakan Desert: Taking Tazhong as example. *Desert Oasis Meteorol.* **2016**, *10*, 36–42. (In Chinese)
10. Gu, Z.L. *Wind-Blown Sand: Near-Surface Turbulence and Gas-Solid Two-Phase Flow*; Science Press: Beijing, China, 2010; Volume 1. (In Chinese)
11. Neakrase, L.D.V.; Balme, M.R.; Esposito, F.; Kelling, T.; Klose, M.; Kok, J.F.; Marticorena, B.; Merrison, J.; Patel, M.; Wurm, G. Particle lifting processes in dust devils. *Space Sci. Rev.* **2016**, *203*, 347–376. [CrossRef]
12. Reiss, D.; Lorenz, R.D.; Balme, M.; Neakrase, L.D.; Rossi, A.P.; Spiga, A.; Zarnecki, J. Dust devils (Space Sciences Series of ISSI). In *Special Issue on Dust Devils*; Springer: Berlin/Heidelberg, Germany, 2017.
13. Freeman, L.H. *Duststorms of the Anglo-Egyptian Sudan*; Meteorological Reports No.11; Great Britain Met. Office Publication: London, UK, 1952.
14. Knippertz, P.; Todd, M.C. Mineral dust aerosols over the Sahara: Processes of emission and transport, and implications for modeling. *Rev. Geophys.* **2009**, *50*, RG1007.

15. Idso, S.B.; Ingram, R.S.; Pritchard, J.M. An American haboob. *Bull. Am. Meteorol. Soc.* **1972**, *53*, 930–935. [CrossRef]
16. Solomos, S.; Kallos, G.; Mavromatidis, E.; Kushta, J. Density currents as a desert dust mobilization mechanism. *Atmos. Chem. Phys.* **2012**, *12*, 11199–11211. [CrossRef]
17. Mamouri, R.E.; Ansmann, A.; Nisantzi, A.; Solomos, S.; Kallos, G.; Hadjimitsis, D.G. Extreme dust storm over the eastern mediterranean in september 2015: Satellite, lidar, and surface observations in the cyprus region. *Atmos. Chem. Phys.* **2016**, *16*, 13711–13724. [CrossRef]
18. Miller, S.D.; Kuciauskas, A.P.; Ming, L.; Qiang, J.; Reid, J.S.; Breed, D.W.; Walker, A.L.; Mandoos, A.A. Haboob dust storms of the southern Arabian Peninsula. *J. Geophys. Res. Atmos.* **2008**, *113*, 1–16. [CrossRef]
19. He, Y.; Gu, Z.; Shui, Q.; Liu, B.; Lu, W.; Zhang, R.; Zhang, D.; Yu, C.W. RANS simulation of local strong sandstorms induced by a cold pool with vorticity. *Atmosphere* **2020**, *11*, 321. [CrossRef]
20. Morman, S.A.; Plumlee, G.S. Dust and human health. In *Mineral Dust*; Knippertz, P., Stuut, J.-B.W., Eds.; Springer: Dordrecht, The Netherlands; Berlin/Heidelberg, Germany; New York, NY, USA; London, UK, 2014; pp. 385–403.
21. Liu, J.T.; Zheng, M.Q. Climatic characteristics of strong and very strong sandstorms in the middle and west parts of inner mongolia. *Plateau Meteorol.* **2003**, *22*, 51–56.
22. Vukovic, A.; Vujadinovic, M.; Pejanovic, G.; Andric, J.; Kumjian, M.R.; Djurdjevic, V.; Dacic, M.; Prasad, A.K.; El-Askary, H.M.; Paris, B.C. Numerical simulation of "An American Haboob". *Atmos. Chem. Phys.* **2014**, *14*, 26175–26215. [CrossRef]
23. Prospero, J.M.; Ginoux, P.; Torres, O.; Nicholson, S.E.; Gill, T.E. Environmental characterization of global sources of atmospheric soil dust identified with the NIMBUS 7 total ozone mapping spectrometer (TOMS) absorbing aerosol product. *Rev. Geophys.* **2002**, *40*, 1–31. [CrossRef]
24. Cowie, S.M.; Knippertz, P.; Marsham, J.H. A climatology of dust emission events from northern Africa using long-term surface observations. *Atmos. Chem. Phys.* **2014**, *14*, 8579–8597. [CrossRef]
25. Allen, C.J.T.; Washington, R.; Engelstaedter, S. Dust emission and transport mechanisms in the central Sahara: Fennec ground-based observations from Bordj Badji Mokhtar, June 2011. *J. Geophys. Res. Atmos.* **2013**, *118*, 6212–6232. [CrossRef]
26. Zender, C.S.; Kwon, E.Y. Regional contrasts in dust emission responses to climate. *J. Geophys. Res. Atmos.* **2005**, *110*, D13201. [CrossRef]
27. Solomos, S.; Ansmann, A.; Mamouri, R.E.; Binietoglou, I.; Patlakas, P.; Marinou, E.; Amiridis, V. Remote sensing and modelling analysis of the extreme dust storm hitting the Middle East and eastern Mediterranean in September 2015. *Atmos. Chem. Phys.* **2017**, *17*, 1–31. [CrossRef]
28. Anisimov, A.; Axisa, D.; Kucera, P.A.; Mostamandi, S.; Stenchikov, G. Observations and cloud-resolving modeling of haboob dust storms over the Arabian Peninsula. *J. Geophys. Res. Atmos.* **2018**, *123*, 12147–12179. [CrossRef]
29. Offer, Z.Y.; Goossens, D. Ten years of aeolian dust dynamics in a desert region (Negev desert, Israel): Analysis of airborne dust concentration, dust accumulation and the high-magnitude dust events. *J. Arid Environ.* **2001**, *47*, 211–249. [CrossRef]
30. Raman, A. Modeling and data analysis of 2011 Phoenix dust storm. In Proceedings of the 93rd AMS Annual Meeting, Austin, TX, USA, 5–10 January 2013.
31. Sutton, L.J. Haboobs. *Q. J. R. Meteorol. Soc.* **1925**, *51*, 25–30. [CrossRef]
32. Bryan, G.H.; Parker, M.D. Observations of a squall line and its near environment using high-frequency rawinsonde launches during VORTEX2. *Mon. Weather Rev.* **2010**, *138*, 4076–4097. [CrossRef]
33. Karam, D.B.; Williams, E.; Janiga, M.A.; Flamant, C.; Mcgrawherdeg, M.; Cuesta, J.; Auby, A.; Thorncroft, C.D. Synoptic-scale dust emissions over the Sahara desert initiated by a moist convective cold pool in early August 2006. *Q. J. R. Meteorol. Soc.* **2014**, *140*, 2591–2607. [CrossRef]
34. Lawson, T.J. Haboob structure at Khartoum. *Weather* **2012**, *26*, 105–112. [CrossRef]
35. Roberts, A.; Knippertz, P. Haboobs: Convectively generated dust storms in West Africa. *Weather* **2012**, *67*, 311–316. [CrossRef]
36. Raman, A.; Arellano, A.F.; Brost, J.J. Revisiting haboobs in the southwestern United States: An observational case study of the 5 July 2011 Phoenix dust storm. *Atmos. Environ.* **2014**, *89*, 179–188. [CrossRef]
37. Li, J. *Weather and Climate in Taklimakan Desert and Surrounding Mountain Areas*; Science Press: Beijing, China, 2003; pp. 164–173. (In Chinese)
38. Huo, W.; Xia, L.I.; Mamtimin, A.; Wang, J.; Zhao, X.C. Analysis on the features of sandstorms in the Tarim Basin in Spring 2004. *Arid Zone Res.* **2006**, *23*, 210–215. (In Chinese)
39. Jiang, X.; Shen, J.; Liu, J.; Chen, S. Observational and numerical simulation of some weather factors leading a severe dust storm. *Acta Meteorol. Sin.* **2003**, *61*, 606–620. (In Chinese)
40. Hu, Y.; Mitsuta, Y. Development of the strong dust storm and dry soluall line—A mechanism analysis on generating black storm. *Plateau Meteorol.* **1996**, *15*, 178–185. (In Chinese)
41. Hu, Y.; Mitsuta, Y. Micrometeorological characteristics and local triggering mechanism of strong dust storm. *Chin. J. Atmos. Sci.* **1997**, *21*, 581–589. (In Chinese)
42. Yang, F.; He, Q.; Huang, J.; Ali, M.; Zheng, W. Desert environment and climate observation network over the Taklimakan Desert. *Bull. Am. Meteorol. Soc.* **2021**, 1–53. [CrossRef]
43. Liu, C.; Cheng, L. Parameterization of the formation and transportion for sand-dust of the black storm and mesoscale numerical experiments. *Acta Meteorol. Sin.* **1997**, *55*, 726–739. (In Chinese)
44. Lu, Q.; Yang, Y.L. *Warnings from Global Dust Storm*; China Environmental Science Press: Beijing, China, 2001; p. 158. (In Chinese)

45. Wang, S.G.; Dong, G.R.; Chen, H.Z.; Li, X.L.; Jin, J. Advances in studying sand-dust storms of China. *J. Desert Res.* **2000**, *20*, 349–356. (In Chinese)
46. Wang, S.; Yang, D.; Jing, J.; Xu, Q.; Yang, Y. Study on the formative causes and countermeasures of the catastrophic sandstorm occurred in northwest China. *J. Desert Res.* **1995**, *15*, 19–30. (In Chinese)
47. Song, Z.; Cheng, L. Diagnostic analysis of the perturbation sources on the "93.5" black storm. *J. Lanzhou Univ.* **1997**, *33*, 116–122. (In Chinese)
48. Zhang, X.; Cheng, L. Diagnosis of vorticity source for the genesis and development of mesoscale vortex during "93.5" black storm. *J. Lanzhou Univ.* **1997**, *33*, 123–131. (In Chinese)
49. Takemi, T. Structure and evolution of a severe squall line over the arid region in northwest China. *Mon. Weather Rev.* **1999**, *127*, 1301–1309. [CrossRef]
50. Takemi, T.; Satomura, T. Numerical experiments on the mechanisms for the development and maintenance of long-lived squall lines in dry environments. *J. Atmos. Sci.* **2000**, *57*, 1718–1740. [CrossRef]
51. Farquharson, J.S. Haboobs and instability in the Sudan. *Q. J. R. Meteorol. Soc.* **2007**, *63*, 393–414. [CrossRef]
52. Ma, Y.; Wang, X.; Xiao, K.; Liu, X.; Tan, J. A case study of a black storm at the northern foothills of Tianshan mountains. *Acta Sci. Nat. Univ. Pekin.* **2006**, *20*, 193–228. (In Chinese)
53. Li, L.; Hu, L.; Liu, W.; Li, Y.; Liang, H. Variation characteristic of main meteorological elements during summer sand- dust storm processes in east of Hexi Corridor. *J. Arid Meteorol.* **2017**, *35*, 427–432. (In Chinese)
54. Zhao, Y. Theoretical Analysis and Numerical Simulations for the Formation, Evolution and Structure of Dust Devil. Ph.D. Thesis, Xi'an Jiaotong University, Xi'an, China, 2004.
55. Scheuvens, D.; Kandler, K. On composition, morphology, and size distribution of airborne mineral dust. In *Mineral Dust*; Knippertz, P., Stuut, J.-B.W., Eds.; Springer: Dordrecht, The Netherlands; Berlin/Heidelberg, Germany; New York, NY, USA; London, UK, 2014.
56. Warner, T.T. *Desert Meteorology*; Cambridge University Press: Cambridge, UK, 2004; p. 612. [CrossRef]
57. Knippertz, P. Meteorological aspects of dust storms. In *Mineral Dust*; Knippertz, P., Stuut, J.-B.W., Eds.; Springer: Dordrecht, The Netherlands; Berlin/Heidelberg, Germany; New York, NY, USA; London, UK, 2014.
58. Knippertz, P.; Trentmann, J.; Seifert, A. High-resolution simulations of convective cold pools over the northwestern Sahara. *J. Geophys. Res. Atmos.* **2009**, *114*, D08110. [CrossRef]
59. Cook, K.H.; Vizy, E.K. Coupled model simulations of the West African monsoon system: Twentieth- and twenty-first-century simulations. *J. Clim.* **2006**, *19*, 3681. [CrossRef]
60. Pantillon, F.; Knippertz, P.; Marsham, J.H.; Panitz, H.-J.; Bischoff-Gauss, I. Modeling haboob dust storms in large-scale weather and climate models. *J. Geophys. Res. Atmos.* **2016**, *121*, 2090–2190. [CrossRef]
61. Roberts, A.J.; Knippertz, P. The formation of a large summertime Saharan dust plume: Convective and synoptic-scale analysis. *J. Geophys. Res. Atmos.* **2014**, *119*, 1766–1785. [CrossRef]
62. Heinold, B.; Knippertz, P.; Marsham, J.H.; Fiedler, S.; Dixon, N.S.; Schepanski, K.; Laurent, B.; Tegen, I. The role of deep convection and nocturnal low-level jets for dust emission in summertime West Africa: Estimates from convection-permitting simulations. *J. Geophys. Res. Atmos.* **2013**, *118*, 4385–4400. [CrossRef]
63. Roberts, A.J.; Woodage, M.J.; Marsham, J.H.; Highwood, E.J.; Ryder, C.L.; Mcginty, W.; Wilson, S.; Crook, J. Can explicit convection improve modelled dust in summertime West Africa? *Atmos. Chem. Phys.* **2018**, *18*, 1–36. [CrossRef]
64. Takemi, T. Explicit simulations of convective-scale transport of mineral dust in severe convective weather. *J. Meteorol. Soc. Jpn. Ser. II* **2004**, *83*, 0076. [CrossRef]
65. Sundram, I.; Claiborn, C.; Strand, T.; Lamb, B.; Chandler, D. Numerical modeling of windblown dust in the Pacific Northwest with improved meteorology and dust emission models. *J. Geophys. Res. Atmos.* **2004**, *109*, 1–12. [CrossRef]
66. Marsham, J.H.; Knippertz, P.; Dixon, N.S.; Parker, D.J.; Lister, G.M.S. The importance of the representation of deep convection for modeled dust-generating winds over West Africa during Summer. *Geophys. Res. Lett.* **2011**, *38*, L16803. [CrossRef]
67. Pope, R.J.; Marsham, J.H.; Knippertz, P.; Brooks, M.E.; Roberts, A.J. Identifying errors in dust models from data assimilation. *Geophys. Res. Lett.* **2016**, *43*, 9270–9279. [CrossRef] [PubMed]
68. Vukovic, A.J.; Pejanovic, G.; Vujadinovic, M.; Sprigg, W.A.; Nickovic, S.; Djurdjevic, V. Dust storm of July 5th 2011, Phoenix, Arizona: Numerical simulation. In Proceedings of the AGU Fall Meeting, San Francisco, CA, USA, 5–9 December 2011.
69. Foroutan, H.; Pleim, J.E. Improving the simulation of convective dust storms in regional-to-global models. *J. Adv. Modeling Earth Syst.* **2017**, *9*, 2046–2060. [CrossRef] [PubMed]
70. Janjic, Z. The step-mountain eta coordinate model: Further development of the convection vicous sublayer and turbulence closure schemes. *Mon. Weather Rev.* **1994**, *122*, 927–945. [CrossRef]
71. Chamberlain, A.C. Roughness length of sea, sand, and snow. *Bound. Layer Meteorol.* **1983**, *25*, 405–409. [CrossRef]
72. Karegar, E.; Hamzeh, N.H.; Jamali, J.B.; Abadi, A.; Goshtasb, H. Numerical simulation of extreme dust storms in east of Iran by the WRF-CHEM model. *Nat. Hazards* **2019**, *99*, 769–796. [CrossRef]
73. Eltahan, M.; Shokr, M.; Sherif, A.O. Tuning dust schemes in weather research forecast (WRF-CHEM) for simulating severe dust storm events over Egypt. *AGU Fall Meet. Abstr.* **2017**, *2017*, A41G-2370.

74. Xue, M.; Droegemeier, K.K.; Wong, V. The Advanced Regional Prediction System (ARPS)—A multi-scale nonhydrostatic atmospheric simulation and prediction model. Part I: Model dynamics and verification. *Meteorol. Atmos. Phys.* **2000**, *75*, 161–193. [CrossRef]
75. Xue, M.; Droegemeier, K.K.; Wong, V.; Shapiro, A.; Brewster, K.; Carr, F.; Weber, D.; Liu, Y.; Wang, D. The Advanced Regional Prediction System (ARPS)—A multi-scale nonhydrostatic atmospheric simulation and prediction tool. Part II: Model physics and applications. *Meteorol. Atmos. Phys.* **2001**, *76*, 143–165. [CrossRef]
76. Song, Z.X. Numerical prediction system for dust weather. In Proceedings of the Annual Meeting of Chinese Meteorological Society, Beijing, China, 18–21 October 2014. (In Chinese).
77. Lu, J.J.; Zhao, L.N.; Du, B.Y. The real time numerical prediction and characteristics of a severe dust storm covers China in the Spring of 2004. *Clim. Environ. Res.* **2007**, *12*, 188–198. (In Chinese)
78. Brown, A.R.; Derbyshire, S.H.; Mason, P.J. Large-eddy simulation of stable atmospheric boundary layers with a revised stochastic subgrid model. *Q. J. R. Meteorol. Soc.* **1994**, *120*, 1485–1512. [CrossRef]
79. Gu, Z.; Jiao, J.; Zhang, Y.; Su, J. The nature of a universal subgrid eddy viscosity model in a turbulent channel flow. *Europhys. Lett.* **2011**, *94*, 34003. [CrossRef]
80. Salim, S.M.; Buccolieri, R.; Chan, A.; Sabatino, S.D. Numerical simulation of atmospheric pollutant dispersion in an urban street canyon: Comparison between RANS and LES. *J. Wind Eng. Ind. Aerodyn.* **2011**, *99*, 103–113. [CrossRef]
81. Versteeg, H.K.; Malalasekera, W. *An Introduction to Computational Fluid Dynamics: The Finite Volume Method*; Pearson Education: London, UK, 2007.
82. Huang, Q.; Marsham, J.H.; Tian, W.; Parker, D.J.; Garcia-Carreras, L. Large-eddy simulation of dust-uplift by a haboob density current. *Atmos. Environ.* **2018**, *179*, 31–39. [CrossRef]
83. McQuaid, J.; Ryder, C.; Sodemann, H.; Garcia-Carreras, L.; Rosenberg, P.; Banks, J.; Brindley, H.; Todd, M.; Engelstaedter, S.; Flamant, C.; et al. Overview and insights gained by airborne observations over the Sahara during Fennec. In Proceedings of the EGU General Assembly 2013, Vienna, Austria, 7–12 April 2013.
84. A Strong Sandstorm Has Hit Jinchang City in Gansu Province, Where Temperatures Have Dropped by 10–15 Degrees Celsius. 2012. Available online: https://weather.mipang.com/shaoxing/news-1809468.html (accessed on 2 March 2021).
85. Lorenz, R.D.; Balme, M.R.; Gu, Z.L.; Kahanpää, H.; Klose, M.; Kurgansky, M.V.; Patel, M.R.; Reiss, D.; Rossi, A.P.; Spiga, A.; et al. History and applications of dust devil studies. *Space Sci. Rev.* **2016**, *203*, 1–33. [CrossRef]
86. Marsham, J.H.; Hobby, M.; Allen, C.J.T.; Banks, J.R.; Bart, M.; Brooks, B.J.; Cavazos-Guerra, C.; Engelstaedter, S.; Gascoyne, M.; Lima, A.R.; et al. Meteorology and dust in the central sahara: Observations from Fennec supersite-1 during the June 2011 intensive observation period. *J. Geophys. Res. Atmos.* **2013**, *118*, 4069–4089. [CrossRef]
87. Metzger, S.M.; Balme, M.; Farrell, W.M.; Fuerstenau, S.; Zarnecki, J. *Resolving Codependent Processes within Natural Dust Devil Vortices*; American Geophysical Union: Washington, DC, USA, 2004.
88. Decroix, D.S.; Lin, Y.L.; Schowalter, D.G. Cellular convection embedded in the convective planetary boundary layer surface layer. *J. Wind Eng. Ind. Aerodyn.* **1997**, *67–68*, 387–401. [CrossRef]
89. Kanak, K.M.; Lilly, D.K.; Snow, J.T. The formation of vertical vortices in the convective boundary layer. *Q. J. R. Meteorol. Soc.* **2010**, *126*, 2789–2810. [CrossRef]
90. Gu, Z.L.; Qiu, J.; Zhao, Y.Z.; Hou, X.P. Analysis on dust devil containing loess dusts of different sizes. *Aerosol Air Qual. Res.* **2008**, *8*, 65–77. [CrossRef]
91. Spiga, A.; Barth, E.; Gu, Z.; Hoffmann, F.; Ito, J.; Jemmett-Smith, B.; Klose, M.; Nishizawa, S.; Raasch, S.; Rafkin, S. Large-eddy simulations of dust devils and convective vortices. *Space Sci. Rev.* **2016**, *203*, 245–275. [CrossRef]
92. Idso, S.B. Dust storms. *Sci. Am.* **1976**, *235*, 108–115. [CrossRef]
93. Gu, Z.; Zhao, Y.; Li, Y.; Yu, Y.; Feng, X. Numerical simulation of dust lifting within dust devils—Simulation of an intense vortex. *J. Atmos. Sci.* **2006**, *63*, 2630–2641. [CrossRef]
94. Gu, Z.L.; Qiu, J.; Zhao, Y.; Li, Y. Simulation of terrestrial dust devil patterns. *Adv. Atmos. Sci.* **2008**, *25*, 31–42. [CrossRef]
95. Johnson, K.L.; Greenwood, J.A. An adhesion map for the contact of elastic spheres. *J. Colloid Interface Sci.* **1997**, *192*, 326. [CrossRef]